Video Article

Visualization of Amyloid β Deposits in the Human Brain with Matrix-assisted Laser Desorption/Ionization Imaging Mass Spectrometry

Masaya Ikegawa*[1], Takashi Nirasawa*[2], Nobuto Kakuda[1], Tomohiro Miyasaka[1], Yuki Kuzuhara[1], Shigeo Murayama[3], Yasuo Ihara[4]

[1]Department of Life and Medical Systems, Doshisha University

[2]Bruker Daltonics K.K.

[3]The Brain Bank for Aging Research, Tokyo Metropolitan Geriatric Hospital and Institute of Gerontology

[4]Graduate School of Brain Science, Doshisha University

*These authors contributed equally

Correspondence to: Masaya Ikegawa at mikegawa@mail.doshisha.ac.jp

URL: https://www.jove.com/video/57645
DOI: doi:10.3791/57645

Keywords: Neuroscience, Issue 145, MALDI-imaging mass spectrometry, human autopsy brain, amyloid β, Alzheimer's disease, senile plaques, cerebral amyloid angiopathy

Date Published: 3/7/2019

Citation: Ikegawa, M., Nirasawa, T., Kakuda, N., Miyasaka, T., Kuzuhara, Y., Murayama, S., Ihara, Y. Visualization of Amyloid β Deposits in the Human Brain with Matrix-assisted Laser Desorption/Ionization Imaging Mass Spectrometry. *J. Vis. Exp.* (145), e57645, doi:10.3791/57645 (2019).

Abstract

The neuropathology of Alzheimer's disease (AD) is characterized by the accumulation and aggregation of amyloid β (Aβ) peptides into extracellular plaques of the brain. The Aβ peptides, composed of 40 amino acids, are generated from amyloid precursor proteins (APP) by β- and γ-secretases. Aβ is deposited not only in cerebral parenchyma but also in leptomeningeal and cerebral vessel walls, known as cerebral amyloid angiopathy (CAA). While a variety of Aβ peptides were identified, the detailed production and distribution of individual Aβ peptides in pathological tissues of AD and CAA have not been fully addressed. Here, we develop a protocol of matrix-assisted laser desorption/ionization-based imaging mass spectrometry (MALDI-IMS) on human autopsy brain tissues to obtain comprehensive protein mapping. For this purpose, human cortical specimens were obtained from the Brain Bank at the Tokyo Metropolitan Institute of Gerontology. Frozen cryosections are cut and transferred to indium-tin-oxide (ITO)-coated glass slides. Spectra are acquired using the MALDI system with a spatial resolution up to 20 µm. Sinapinic acid (SA) is uniformly deposited on the slide using either an automatic or a manual sprayer. With the current technical advantages of MALDI-IMS, a typical data set of various Aβ species within the same sections of human autopsied brains can be obtained without specific probes. Furthermore, high-resolution (20 µm) imaging of an AD brain and severe CAA sample clearly shows that Aβ1-36 to Aβ1-41 were deposited into leptomeningeal vessels, while Aβ1-42 and Aβ1-43 were deposited in cerebral parenchyma as senile plaque (SP). It is feasible to adopt MALDI-IMS as a standard approach in combination with clinical, genetic, and pathological observations in understanding the pathology of AD, CAA, and other neurological diseases based on the current strategy.

Video Link

The video component of this article can be found at https://www.jove.com/video/57645/

Introduction

In order to make the diagnosis and to understand the pathogenesis of neurodegenerative disorders, precise molecular identification of pathological deposits is essential[1]. In the course of AD, Aβ is produced to make SPs in the cerebral parenchyma and deposited in vessels long before disease onset[2,3,4,5,6]. While Aβ1-42 is the predominant peptide in the SP of AD brains, other Aβ variants, such as N-terminal or C-terminal truncated or modified Aβs, are also identified in affected AD brains[7,8,9,10]. A full picture of the broad range of Aβ species in human brains, especially with AD and cerebral amyloid angiopathy (CAA)[11], will help scientists understand Aβ production, metabolism, and deposition.

As the classical approach of neuropathology, immunohistochemistry (IHC) has been the most conclusive method to determine the location of Aβs in the brain tissues[12,13,14,15]. In general, IHC cannot distinguish molecules when several epitopes coexist simultaneously. By contrast, an emerging mass spectrometry-based proteomic analysis is a valuable approach especially for analyzing a variety of Aβ species in brain tissues, which cannot be differentiated with antibodies[16,17]. The conventional mass spectrometry-based analysis of brain lysates and immuno-precipitated samples fails to detect minor Aβ peptides and loses distribution information of Aβ in the brain tissue.

In earlier works, visualizing Aβ deposits in mouse brains has been successful using a transgenic animal model of AD, such as APP23. However, this process still needs technical advancements to compare IMS and IHC with respect to resolution and sensitivity[18,19,20]. AD neuropathology should be studied on human brains, and we used MALDI-IMS technology on human autopsy brain tissues to obtain comprehensive protein mapping[21]. For this purpose, we developed a protocol for an advanced type of mass spectrometry that has advantages in its rapidity, sensitivity, and reproducibility.

Protocol

Here, tissue samples were collected at the Tokyo Metropolitan Geriatric Hospital, which provides community-based medical services to the elderly population in Japan. The brain autopsy samples used in the study were registered to the Brain Bank for Aging Research (BBAR) with the informed consent of the deceased's relatives. The BBAR is approved by the ethics committee of the Tokyo Metropolitan Geriatric Hospital and Institute of Gerontology. For all brains registered at the brain bank, we obtained written informed consents for their use for medical research from the patients or their families. The patients were placed in a cold (4 °C) room within 2 h after death to reduce postmortem changes in the brain. All methods described here have been approved by Doshisha University and the Brain Bank for Aging Research, Tokyo Metropolitan Geriatric Hospital and Institute of Gerontology.

1. Preparation of Tissue Sections for IMS

1. **Processing tissue specimen of a human autopsied brain**
   Note: Ensure that the sample preparation step for IMS preserves the original state of the tissue. Avoid contamination and post-mortem changes. The following step is crucial.
   1. Obtain human cortical specimens for IMS from brains that were removed, processed, and stored at -80 °C within 8 h postmortem. Take the brain specimen from the occipital cortex of AD patients and age-matched controls[21].

2. **Preparation of frozen tissue sections**
   1. Cut the tissue sections on a cryostat. Place conductive ITO-coated microscope glass slides inside the cryostat[21].
   2. Warm the autopsy brain specimen from -80 °C to -22 °C inside the cryostat.
   3. Attach a new disposable blade to the cryostat for every experiment. Always try to use a clean part of the blade.
   4. Put the frozen autopsy brains on the stage along with a small amount of OCT compound (enough to cover the central area of the stage; see **Table of Materials**).
   5. Choose the conditions for thin sectioning. For IMS, use a thickness of 10–12 µm for human brain sections. For IMS and IHC, cut five to six sections from each tissue sample.
   6. When the blade is just starting to cut the tissue, turn the wheel and "face" the block until all of the tissue is exposed. If there is a small streak or tear across the section, wait a little more in the cryostat until the temperature adjustment automatically fixes it. Count a few seconds before opening the anti-roll with a tissue underneath.
   7. Immediately place the tissue slice on the ITO-coated side of the glass slide. Thaw the tissue slice by putting a finger underneath the slide on the non-ITO-coated side. The tissue will stick to the slide; ensure that the tissue is as flat as possible with no wrinkles. Perform this step at room temperature.
      Note: Wear gloves, masks, and a laboratory gown because the human samples may contain biological contaminants. When all sections have been made for the day, clean the cryostat, brushes, and chucks with laboratory wipes and 200 mL of 100% ethanol.

3. **Rinsing the tissue sections**
   1. Immerse the samples in 40–100 mL of 70% ethanol for 30 s to remove endogenous lipids and inorganic salts. Use a glass staining jar.
   2. Wash the samples with 40–100 mL of 100% ethanol for 30 s, 40–100 mL of Carnoy's solution for 3 min, 40–100 mL of 100% ethanol for 30 s, 40–100 mL of 0.1% trifluoroacetic acid (TFA) for 1 min, and 40–100 mL of 100% ethanol for 30 s. Use a glass staining jar.
      Note: Carnoy's solution is a fixative composed of six parts ethanol, three parts acetic acid, and one part chloroform.
   3. Dry in a vacuum for 30 min.

4. **Treatment of the tissue sections with a formic acid vapor for a better ionization of the Aβ proteins from autopsy brain tissues**
   1. Prepare the oven and incubation glass slide to be used for the subsequent vaporization with 5 mL of 100% formic acid. To achieve a satisfactory acid treatment, keep the air humidity in the incubation glass dish at saturation level throughout this step and keep the temperature at 60 °C. Place the tissue slides in the incubation glass dish while avoiding submersion in the formic acid and treat for 6 min.
   2. Take an optical image of the samples using a film scanner, gel scanner, or a digital microscope, *etc.* Perform this step at room temperature. The alignment of the optical image of the samples is necessary when the sample target is placed inside the instrument. Usually, it will not be possible to recognize the tissue section underneath the matrix layer.
      NOTE: The most convenient way to take an optical image is to use an office scanner. It is a good idea to save the image in the imaging data storage folder.
   3. To correlate the optical images with the samples, make guide marks that are visible both in the optical image and underneath the matrix layer in the camera optic. The easiest way is to spot at least three correction fluid marks around the sample before taking the optical image.

5. **Matrix application**
   1. **Preparation of the matrix solution**
      1. In an organic solvent-tolerant microtube, prepare a 10 mg/mL SA solution in 50% acetonitrile (ACN) and 0.1% TFA. Thoroughly dissolve the SA compound by vortexing or brief sonication for 10 min. Store the solution at room temperature until use.
         NOTE: There are three different options for matrix spraying: using an airbrush, an ultrasonic sprayer, or an automatic sprayer.

   2. **Spraying the matrix with an airbrush**
      1. Perform the operation at a constant room temperature (20–23 °C) and humidity (40%–60%). The parameters to adjust for optimal spraying include the size of the droplet, the amount of mist, the angle and distance between the spray nozzle and the tissue section, and the laboratory temperature and humidity. Adjust these conditions by checking the microscopy results.

Note: As limiting factors include the crystal size and homogeneity of the matrix coverage and the undesirable migration/diffusion of analytes, smaller is better for the drop size. Homogeneity is also the point of inspection.

3. **Spraying the matrix with an ultrasonic sprayer**
    1. Remove the tissue to be sprayed from the desiccator and place it in the chamber. Make sure the tissue is not covering the sensor window.
    2. Start the preparation by pushing the **Start** button; usually, prep time is around 90 min. The preparation will be regulated automatically via the monitoring of the matrix layer thickness and wetness. After the preparation is complete, remove the slide and store it in the desiccator for 15 min before reading it in the MALDI instrument.
    3. Clean the sprayer with 2–3 mL of 100% MeOH until the spray head appears clean.
    Note: A fine mist of matrix droplets is allowed to sink into the tissue by a gravitational sheet. An average droplet size of 20 µm is generated; all droplet diameters are less than 50 µm.

4. **Spraying the matrix with an automatic sprayer**
    1. Spray the matrix solution on the tissue surface with an automatic sprayer. A constant flow of heated sheath gas (N2, set at 10 psi and 75 °C) will be delivered conjointly with the matrix solution spray. Use a solvent pump system (set at 10 psi and 0.15 mL/min) to deliver the matrix solution.
    Note: Most importantly, work under a safety cabinet to avoid any inhalation of matrix aerosols. Control the room temperature and humidity to reproduce homogenous matrix crystallization.

2. MALDI-IMS

1. **Perform ultra-high-speed mass spectrometry.**
    1. Perform high-throughput and high-spatial-resolution imaging experiments with MALDI-IMS equipped with a 10 kHz Nd:YAG (355 nm) laser.
    2. For mass spectrometry measurements, define the tissue areas using the MALDI control software and data analysis software.
    3. Acquire spectra in a positive linear mode with a mass range of m/z 2,000–20,000 and a spatial resolution of 20 and 100 µm.
    4. To make the calibration standard, dissolve the peptide calibration standard and the protein calibration standard with a ratio of 1:4 with alpha-Cyano-4-hydroxyl-cinnamic acid (CHCA) in TA30 solution (ACN:0.1% TFA = 30:70) and then dilute it 10x. Place 1 µL of calibration standard on the slide at four different locations.

2. Using molecular histology software (see **Table of Materials**), overlay multiple single images to find the spatial correlation of various signals, such as different Aβ peptides colocalizing in SPs and arterial walls.

3. Data Processing

1. For spectral alignment, align all spectra to a selected m/z list from a previous publication[21].
2. Import the MALDI-IMS data set into statistical analysis software (see **Table of Materials**) with baseline subtraction.
3. **Trace regions of interest (ROIs) based on histological knowledge.**
    1. Perform a univariate analysis for the mean intensities, standard deviations, uncovering of discriminative m/z-markers (ROC analysis), hypothesis tests, and discovery of colocalized m/z values.

4. **Create a segmentation map.**
    1. Perform an unsupervised multivariate analysis for the spatial segmentation of large datasets and a component analysis for the extraction of underlying trends.
    2. Select anatomical ROIs based on histological characteristics, such as parenchyma and the subarachnoid space.
    3. Assign structures as individual ROIs and correlate them with the processed MS data in order to identify the associated peptides that allowed the image segmentation of the region.

Representative Results

Sporadic AD patients with CAA (*n* = 5; mean age = 83.2 y) and aged subjects with senile plaque free (SP O) and CAA (*n* = 5; mean age = 77.2 y) were analyzed (**Table 1**). The CAA phenotypes of patient #3 were most prominent in this study. Distributions of Aβ1-40 and Aβ1-42 deposits in the brain tissue from patient #3 were visualized with MALDI-IMS (**Figure 1**). There were no significant signals in nonpathological control brains (patients #9 and #10), as shown in **Figure 1**. Here, MALDI-IMS clearly visualized that Aβ1-42 was preferentially deposited as SPs in the cerebral parenchyma. By contrast, shorter Aβs, such as Aβ1-36 to 1-41, were preferentially deposited on the leptomeningeal vascular areas (**Figure 1**).

Distributions of Aβ40 and Aβ42 were further validated with IHC using adjacent frozen sections of the tissues. The anti-Aβ40 antibody labeled CAA (arrows in **Figure 2B**), which is in clear contrast to the distribution of Aβ42 in the cerebral parenchyma as SPs. For Aβ1-41, we are the first to detect this fragment in human brains, and we have generated specific antibodies that can differentiate Aβ41 from Aβ40 andAβ42[21].

The spatial resolution of the MALDI-IMS is generally the most important factor to be improved upon. In **Figure 1** and **Figure 2** show MALDI-IMS with a 100 µm pitch resolution and obtain an overall distribution profile for a relatively wide area[21]. It is difficult to define amyloid deposition exactly at the subarachnoid space, including vascular structure. To portray fine tissue structures of subarachnoid vessels and the surface of the cortex, high-resolution MALDI imaging (40 µm: **Figure 3**; 20 µm: **Figure 4** and **Figure 5**) was performed. As a result, MALDI-IMS clearly demonstrated that shorter Aβs, such as Aβ1-36 to 1-41, are distributed in the walls of arteries, which is comparable with IHC.

MALDI-IMS demonstrated the detailed distributions of both Aβx-40 and Aβx-42 (x = 2, 4, 5, 6, 7, 8, 9, and 11pE) in AD accompanied with moderate CAA brain. For example, while Aβx-40 species showed a similar distribution profile to Aβ1-40, Aβx-42 species showed a different distribution pattern with Aβ1-42[21]. By the current protocol, single ion images of the individual Aβ peptides observed with MALDI-IMS are assigned to Aβ species. By contrast, acquired image data can be investigated using unsupervised multivariate statistics in order to obtain image segmentation of anatomical regions of interest for the further analysis of undefined proteins. **Figure 5** shows a segmentation map obtained with a bisecting k-means analysis applied to the same section from patient #3[21]. This clustering method successfully identified plaque-like structures in the parenchyma (blue in **Figure 5C**) and vascular structures in the subarachnoid space (green in **Figure 5C**). It is interesting to find a small circular area in the parenchyma, which is detected just around a small arteriole in the parenchyma, as well as in the subarachnoid space (purple in **Figure 5C**). This is verified by single ion images of these individual Aβ peptides in **Figure 5D-5F**.

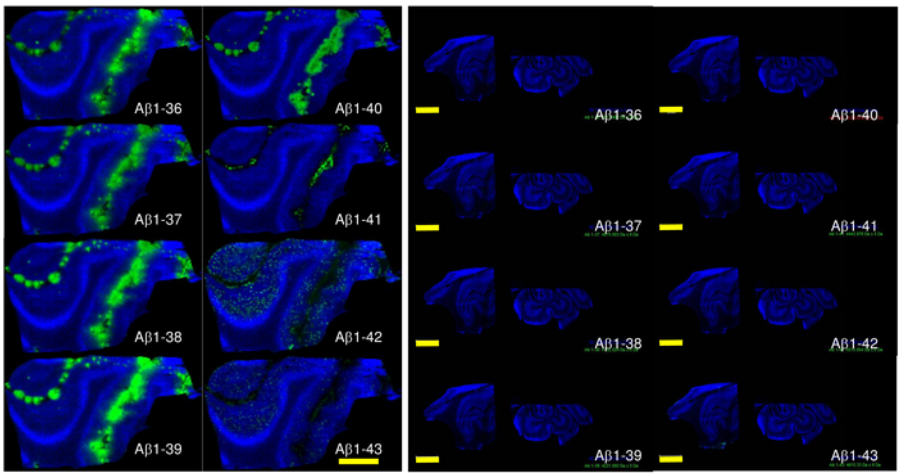

Figure 1: MALDI-IMS of a frozen AD/CAA brain section. Various C-terminal truncated Aβ peptides in AD accompanying severe CAA (patient #3) are visualized in the left panel and controls (patient #9 on the right and patient #10 on the left in all images) in the right panel. Aβ1-36 to Aβ1-41 are preferentially deposited in leptomeningeal blood vessels, while Aβ1-42 and Aβ1-43 are deposited in the cerebral parenchyma as senile plaques in case #3, while there was no signal in the control patients' brains (cases #9 and #10). Resolution = 100 µm. Scale bar = 5 mm. This figure has been modified with permission from Kakuda et al.[21]. Please click here to view a larger version of this figure.

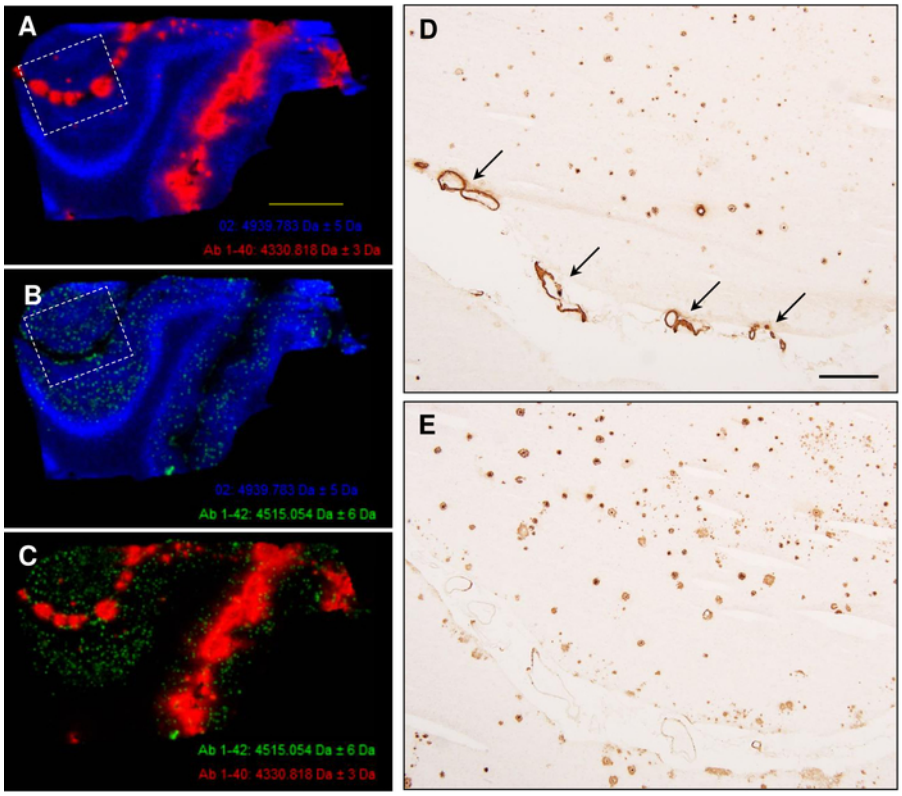

Figure 2: MALDI-IMS of frozen AD/CAA brain sections and adjacent sections of the occipital cortex from AD brains. (**A** - **C**) The frozen AD/CAA brain sections and (**D** and **E**) adjacent sections of the occipital cortex from AD brains were immune-stained and focused on arteriole and cerebral parenchyma, using antibodies against Aβ40 (**D:** BA27) or Aβ42 (**E**: anti-Aβ42 polyclonal). Both analyses demonstrated that Aβ40 is preferentially deposited in leptomeningeal blood vessels (arrows in panel **D**) and arterioles in the subarachnoid space and the cerebral parenchyma forming CAA. In contrast, Aβ42 is mainly deposited in SPs. For IMS, Resolution = 100 µm. Scale bar = 5 mm (**A**, **B**, and **C**) = 5 mm, 500 (**D** and **E**). This figure has been modified with permission from Kakuda et al.[21]. Please click here to view a larger version of this figure.

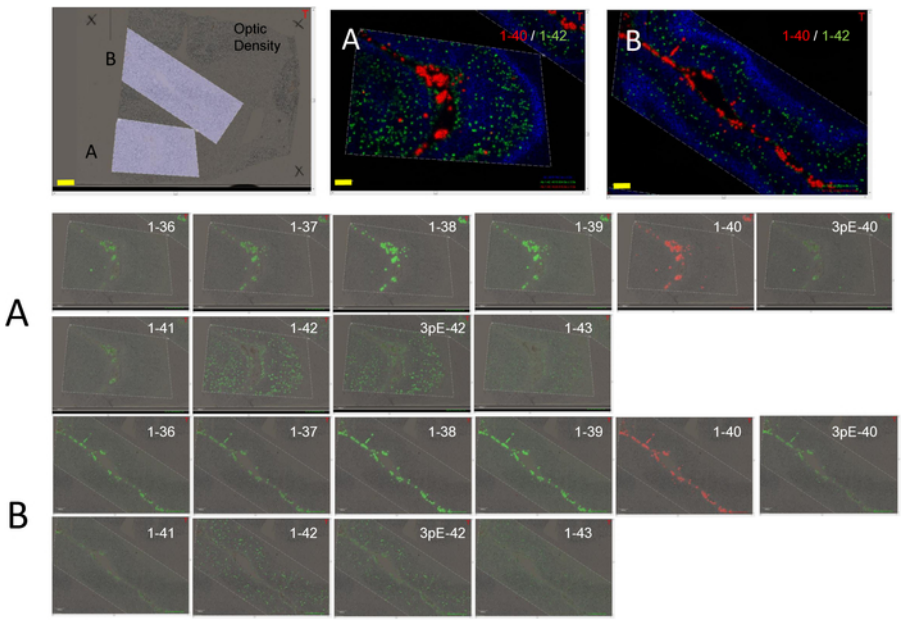

Figure 3: MALD-IMS of frozen AD/CAA brain sections (patient #3) at a resolution of 40 µm. Various C-terminal and N-terminal truncated and modified Aβ peptides in AD accompanying severe CAA (patient #3). Aβ1-36 to Aβ1-41 are preferentially deposited in leptomeningeal blood vessels, while Aβ1-42 and Aβ1-43 are deposited in the cerebral parenchyma as senile plaques. Scale bars = 1 mm (A-B), 2 mm (upper left). Resolution = 40 µm. Please click here to view a larger version of this figure.

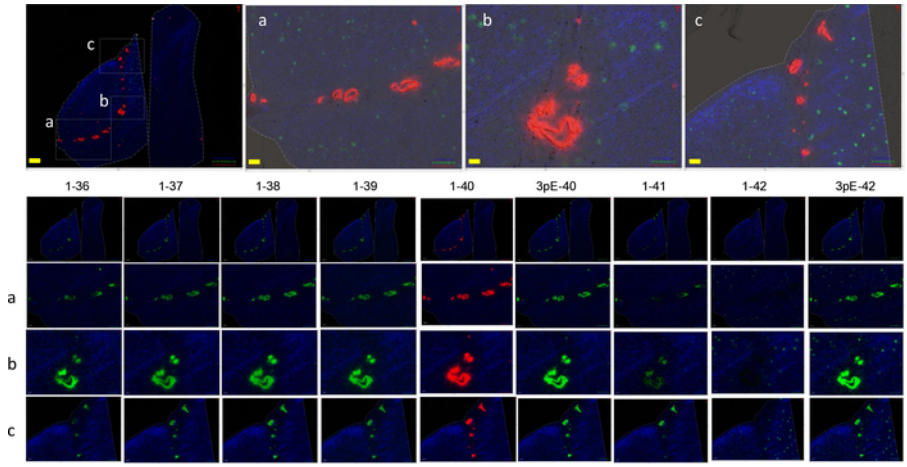

Figure 4: MALDI-IMS of frozen AD/CAA brain sections (patient #3) at a resolution of 20 µm. This panel shows various C-terminal and N-terminal truncated and modified Aβ peptides in AD accompanying severe CAA (patient #3). Aβ1-36 to Aβ1-41 are preferentially deposited in leptomeningeal blood vessels, while Aβ1-42 and Aβ1-43 are deposited in the cerebral parenchyma as senile plaques. Scale bars = 200 µm (a, b, c), 1 mm (upper left). Resolution = 20 µm. Please click here to view a larger version of this figure.

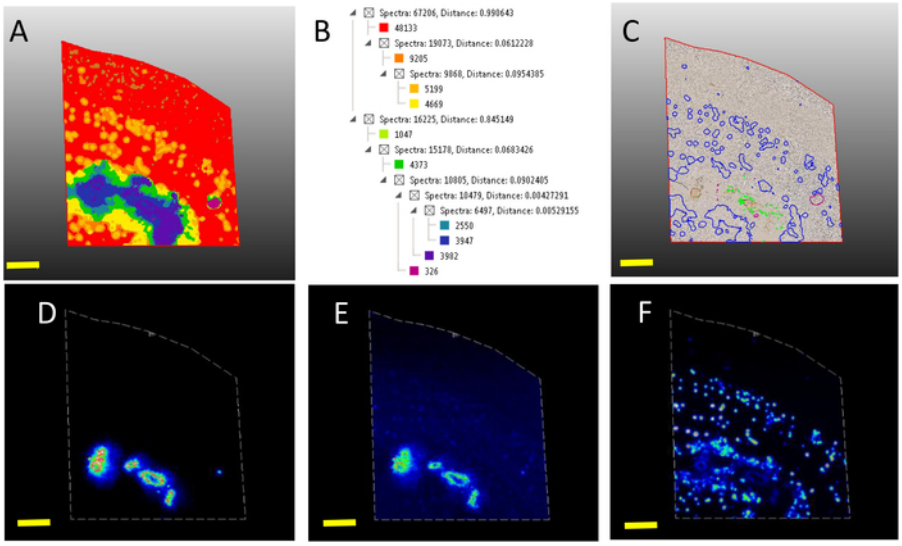

Figure 5: Segmentation map, obtained by MALDI-IMS of a frozen AD brain section, reveals putative senile plaque, large subarachnoid vessel structures, and small parenchymal arterioles. (**A**) Segmentation map obtained from a multivariate image analysis of MALDI-IMS data. (**B**) Bisecting k-means based clustering analysis identified plaque-like and vessel-like structures in the occipital cortex. The clusters and substructures and their relations are shown as nodes (e.g.,1-0-0). (**C**) Distinct Aβ peptide localization patterns resembling plaques (blue), subarachnoid vessels (green), and arteriole (red) structures. Note that a few red clusters are also distributed in the subarachnoid space. This is verified by single ion images of these individual Aβ peptides at a 20 µm resolution: (**D**) Aβ 1-40, (**E**) Aβ 1-41, and (**F**) Aβ 1-42. Please click here to view a larger version of this figure.

Case	Gender	Age at death	Braak SP	CAA
1	M	83	C	0.5
2	M	88	C	1
3	M	84	C	2
4	M	78	C	1
5	M	83	C	1
6	M	84	O	0
7	M	78	O	0
8	M	70	O	0
9	M	73	O	0
10	M	81	O	0

Table 1: Clinical and pathological data of AD with CAA cases and aged SP O subjects. Human cortical specimens for IMS and IHC were obtained from the Brain Bank at Tokyo Metropolitan Institute of Gerontology. Each brain specimen was taken from the occipital cortex of five AD patients and five age-matched controls. The extent of amyloid deposition as shown by an Aβ monoclonal antibody was defined by Braak SP (amyloid) stages. At stage O, there are almost no senile plaques throughout the isocortex. At stage C, virtually all the isocortical areas are affected. AD brains are invariable at stage C. This table has been modified with permission from Kakuda et al.[21].

Discussion

Here we demonstrated a detailed protocol and results of the visualization of Aβ and its isoforms from several autopsied brains with AD and CAA with MALDI-IMS. The deposition profile of Aβs was drastically changed from Aβ1-42 to its N- and C-terminal variations. Aβ1-41 was first identified and visualized in human brains with the current protocol and was further validated with IHC[21]. Considering that the morphology of deposited Aβ by IMS with a high-resolution analysis (20 μm) must be in good agreement with IHC, IMS and IHC equally contribute to distinguishing Aβ deposits by their location and protein contents, as well as by their morphology. As the entire experiment described here was conducted in the occipital cortex, studying the localization of different beta-amyloid species across all brain regions will be generalized with future experiments using the current protocol.

Critical steps within the protocol are tissue preparation steps to obtain an effective ionization of aggregated proteins in human brain tissues. A matrix layer is required to absorb the laser energy and induce desorption and ionization of analytes. In this process, an entire tissue section is homogeneously coated with small crystals. Homogenous cocrystallization of the analyte with the matrix is crucial for high-sensitivity and artifact-free imaging. Each of the three spray methods has its own advantages. Manual spray coating is one of the most frequently used methods. An airbrush is convenient; however, it requires skillful operation. As precise and reproducible experimental technique is essential, using an ultrasonic sprayer and/or an automatic sprayer as described in the current protocols is recommended. With respect to an ultrasonic sprayer, it will not be influenced by the humidity and temperature of the room because it is sprayed into a chamber. Meanwhile, with an automatic sprayer, relatively preserved spatial resolution with good reproducibility is obtained. Generally, the spatial resolution obtained with the three methods increase in the order of 1) airbrush, 2) automatic device, and 3) ultrasonic sprayer.

Most importantly, this protocol was originally generated to detect and visualize Aβs in human autopsied brain samples. The visualization of Aβs with MALDI-IMS for APP23 mice, which is generated as an animal model of AD based on the Swedish-type mutation of human APP, has been reported earlier by others with an existing method[18,19]. However, the former protocol applied to APP23 was not sufficient to visualize Aβ in its lateral resolution and sensitivity. Earlier works discussed that high Aβ concentrations outside the tissue boundary are clearly artifacts in APP23 imaging with their protocol[18,19]. That means the so-called 'blur' between real SPs and IMS images due to the matrix extraction step was inevitable with MALDI-type imaging. However, in the current protocol, the blur disappeared and each spectrum represented every single SP in the brain parenchyma.

As shown here, we can trace Aβ1-41 for the first time in AD and CAA brains with MALDI-IMS, as well as with IHC, with a specific antibody by our own generation[21]. According to the Aβ processing model, Aβ1-38 derives from Aβ1-45 *via* Aβ1-42, while Aβ1-41 derives from Aβ1-45 by γ-secretase stepwise cleavage[27,28,29,30,31]. This means that the current protocol supports this model. As for the limitations of this technique, we must consider the heterogeneity of the samples from human autopsy brain. The most critical step, in a sense, is to assess qualified autopsy brain tissue with ethical proof. With the current protocol on those qualified autopsy brain tissues, MALDI-IMS can individually track the whole distribution of the complex molecules having multiple modifications, as well as unknown factor(s) regulating the pathogenesis of AD, that are yet to be defined. Furthermore, in understanding the overall pathogenesis of various neuropathology in aged human brains, it must be feasible to adopt MALDI-IMS as a standard approach, in combination with clinical, genetic, and pathological observations in neurological diseases.

Another critical step of MALDI-IMS is the data mining process from the obtained data set, which is always time-consuming. Manual data mining of each peak distribution requires the users to click through every image and look for distributions that may correlate to the morphology of the analyzed sample. Automatic spatial segmentation can be used as the first step of data mining, providing an overview of the data set and allowing the quick detection of prominent features. In this approach, similarities between spectra of a given region are statistically determined, and similar spectra are grouped into one cluster. All pixels are color-coded according to their cluster assignment (**Figure 5**). In the present AD/CAA study, the area of interest is the space of Aβ depositions in parenchymal plaque and the subarachnoid and parenchymal vascular structures. The two distinctive peaks which were further validated with IHC were the m/z values from Aβ1-40 and Aβ1-42[21]. Thus, it is easy to find colocalized m/z with Aβ1-40 and Aβ1-42 which was already annotated to N- and C-terminal truncated Aβ, as well as unknown peptides, for further analysis.

Weller and colleagues have reported that Aβ accumulates in vessel walls, more around arteries than around veins[21]. Moreover, it has been proposed that the interstitial fluid (ISF) includes Aβs excreted from the cerebral parenchyma to the lymph node *via* a perivascular drainage pathway[22,23,24,25,26]. The current protocol to generate a segmentation map based on a MALDI-IMS data set at a 20 µm resolution supports the possible existence of perivascular drainage pathways of the brain (**Figure 5**), which contribute significantly to CAA in AD[21,32]. Furthermore, we can discover marker proteins colocalized with plaque and subarachnoid vasculature by calculating the correlation of each m/z values. In understanding the overall pathogenesis of various neuropathology in aged human brains, it must be feasible to adopt MALDI-IMS as a powerful approach in combination with established IHC data of clinical, genetic, and pathological observations in neurological diseases.

Disclosures

The authors have nothing to disclose.

Acknowledgments

This work was supported in part by the Grant-in-Aid for Scientific Research on Innovative Areas (Brain Protein Aging and Dementia Control 26117004; to M.I. and T.M.). This research was partially supported by the Strategic Research Program for Brain Sciences from the Japan Agency for Medical Research and Development (AMED). All experiments were conducted in compliance with the ARRIVE guidelines.

References

1. Kovacs, G.G. Molecular Pathological Classification of Neurodegenerative Diseases: Turning towards Precision Medicine. *International Journal of Molecular Sciences.* **17**, E189 (2016).
2. Selkoe, D.J. Alzheimer's disease: genes, proteins, and therapy. *Physiological Reviews.* **81**, 741-766 (2001).
3. Selkoe, D.J., Hardy, J. The amyloid hypothesis of Alzheimer's disease at 25 years. *EMBO Molecular Medicine.* **8**, 595-608 (2016).
4. Braak, H., Braak, E. Neuropathological stageing of Alzheimer-related changes. *Acta Neuropathologica.* **82**, 239-259 (1991).
5. Braak, H., Alafuzoff, I., Arzberger, T., Kretzschmar, H., Del Tredici, K. Staging of Alzheimer disease-associated neurofibrillary pathology using paraffin sections and immunocytochemistry. *Acta Neuropathologica.* **112**, 389-404 (2006).
6. Bateman, R.J. *et al.* Dominantly Inherited Alzheimer Network. Clinical and biomarker changes in dominantly inherited Alzheimer's disease. *The New England Journal of Medicine.* **367**, 795-804 (2012).
7. Iwatsubo, T. *et al.* Visualization of A beta 42(43) and A beta 40 in senile plaques with end-specific A beta monoclonals: evidence that an initially deposited species is Abeta 42(43). *Neuron.* **13**, 45-53 (1994).
8. Reinert, J. *et al.* Deposition of C-terminally truncated Aβ species Aβ37 and Aβ39 in Alzheimer's disease and transgenic mouse models. *Acta Neuropathologica Communications.* **4**, 24 (2016).
9. Saido, T.C. *et al.* Dominant and differential deposition of distinct beta-amyloid peptide species, A beta N3(pE), in senile plaques. *Neuron.* **14**, 457-466 (1995).
10. Harigaya, Y. *et al.* Amyloid beta protein starting pyroglutamate at position 3 is a major component of the amyloid deposits in the Alzheimer's disease brain. *Biochemical and Biophysical Research Communications.* **276**, 422-427 (2000).
11. Vinters, H.V. Cerebral amyloid angiopathy. A critical review. *Stroke.* **18**, 311-324 (1987).
12. Saito, T. *et al.* Potent amyloidogenicity and pathogenicity of Aβ43. *Nature Neuroscience.* **14**, 1023-1032 (2011).
13. Sergeant, N. *et al.* Truncated beta-amyloid peptide species in pre-clinical Alzheimer's disease as new targets for the vaccination approach. *Journal of Neurochemistry.* **85**, 1581-1591 (2003).
14. Suzuki, N. *et al.* High tissue content of soluble beta 1-40 is linked to cerebral amyloid angiopathy. *The American Journal of Pathology.* **145** (2), 452-460 (1994).
15. Miyasaka, T. *et al.* Visualization of newly deposited tau in neurofibrillary tangles and neuropil threads. *Journal of Neuropathology & Experimental Neurology.* **64**, 665-674 (2005).
16. Portelius, E. *et al.* Mass spectrometric characterization of brain amyloid beta isoform signatures in familial and sporadic Alzheimer's disease. *Acta Neuropathologica.* **120**, 185-193 (2010).
17. Kelley, A.R., Perry, G., Castellani, R.J., Bach, S.B. Laser-Induced In-Source Decay Applied to the Determination of Amyloid-Beta in Alzheimer's Brains. *ACS Chemical Neuroscience.* **7**, 261-268 (2016).
18. Stoeckli, M., Staab, D., Staufenbiel, M., Wiederhold, K.H., Signor, L. Molecular imaging of amyloid beta peptides in mouse brain sections using mass spectrometry. *Analytical Biochemistry.* **311**, 33-39 (2002).
19. Stoeckli, M. *et al.* MALDI MS imaging of amyloid. *Methods in Enzymology.* **412**, 94-106 (2006).
20. Seeley, E.H., Caprioli, R.M. Molecular imaging of proteins in tissues by mass spectrometry. *Proceedings of the National Academy of Sciences of the United States of America.* **105**, 18126-18131 (2008).
21. Kakuda, N. *et al.* Distinct deposition of amyloid-β species in brains with Alzheimer's disease pathology visualized with MALDI imaging mass spectrometry. *Acta Neuropathologica Communications.* **5**, 73 (2017).
22. Weller, R.O., Djuanda, E., Yow, H.Y., Carare, R.O. Lymphatic drainage of the brain and the pathophysiology of neurological disease. *Acta Neuropathologica.* **117**, 1-14 (2009).
23. Weller, R.O., Boche, D., Nicoll, J.A. Microvasculature changes and cerebral amyloid angiopathy in Alzheimer's disease and their potential impact on therapy. *Acta Neuropathologica.* **118**, 87-102 (2009).
24. Weller, R.O., Subash, M., Preston, S.D., Mazanti, I., Carare, R.O. Perivascular drainage of amyloid-beta peptides from the brain and its failure in cerebral amyloid angiopathy and Alzheimer's disease. *Brain Pathology.* **18**, 253-266 (2008).
25. Morris, A.W. *et al.* Vascular basement membranes as pathways for the passage of fluid into and out of the brain. *Acta Neuropathologica.* **131**, 725-736 (2016).
26. Hawkes, C.A. *et al.* Perivascular drainage of solutes is impaired in the ageing mouse brain and in the presence of cerebral amyloid angiopathy. *Acta Neuropathologica.* **121**, 431-443 (2011).

27. Kakuda, N. *et al.* Equimolar production of amyloid beta-protein and amyloid precursor protein intracellular domain from beta-carboxyl-terminal fragment by gamma-secretase. *Journal of Biological Chemistry.* **281**, 14776-14786 (2006).
28. Matsumura, N. *et al.* γ-Secretase associated with lipid rafts: multiple interactive pathways in the stepwise processing of β-carboxyl-terminal fragment. *Journal of Biological Chemistry.* **289**, 5109-5121 (2014).
29. Morishima-Kawashima, M. *et al.* Effect of apolipoprotein E allele epsilon4 on the initial phase of amyloid beta-protein accumulation in the human brain. *The American Journal of Pathology.* **157**, 2093-2099 (2000).
30. Takami, M. *et al.* γ-Secretase: Successive tripeptide and tetrapeptide release from the transmembrane domain of β-carboxyl terminal fragment. *The Journal of Neuroscience.* **29**, 13042-13052 (2009).
31. Kakuda, N. *et al.* Altered γ-secretase activity in mild cognitive impairment and Alzheimer's disease. *EMBO Molecular Medicine.* **4**, 344-352 (2012).
32. Carlred, L. *et al.* Probing amyloid-b pathology in transgenic Alzheimer's disease (tgArcSwe) mice using MALDI imaging mass spectrometry. *Journal of Neurochemistry.* **138**, 469-478 (2016).